REVIEW OF SCIENTIFIC INSTRUMENTS **84**, 056107 (2013)

Note: Operation of gamma-ray microcalorimeters at elevated count rates using filters with constraints

B. K. Alpert,[1] R. D. Horansky,[1] D. A. Bennett,[1] W. B. Doriese,[1] J. W. Fowler,[1]
A. S. Hoover,[2] M. W. Rabin,[2] and J. N. Ullom[1]
[1]*National Institute of Standards and Technology, Boulder, Colorado 80305, USA*
[2]*Los Alamos National Laboratory, Los Alamos, New Mexico 87545, USA*

(Received 21 March 2013; accepted 29 April 2013; published online 15 May 2013)

Microcalorimeter sensors operated near 0.1 K can measure the energy of individual x- and gamma-ray photons with significantly more precision than conventional semiconductor technologies. Both microcalorimeter arrays and higher per pixel count rates are desirable to increase the total throughput of spectrometers based on these devices. The millisecond recovery time of gamma-ray microcalorimeters and the resulting pulse pileup are significant obstacles to high per pixel count rates. Here, we demonstrate operation of a microcalorimeter detector at elevated count rates by use of convolution filters designed to be orthogonal to the exponential tail of a preceding pulse. These filters allow operation at 50% higher count rates than conventional filters while largely preserving sensor energy resolution. © *2013 AIP Publishing LLC*. [http://dx.doi.org/10.1063/1.4806802]

Microcalorimeter sensors have demonstrated energy resolutions as good as 22 eV full-width-at-half-maximum for 97 keV gamma-rays, roughly 20 times better than state-of-the-art planar germanium sensors.[1] These microcalorimeters rely on superconducting transition-edge sensor (TES) thermometers and derive their exquisite energy resolution from the low thermal noise at typical operating temperatures near 0.1 K. While the collecting area of individual elements is small ($\sim$2 mm^2), the total active area of emerging microcalorimeter arrays is comparable to that of planar germanium sensors ($\sim$5 cm^2) thus making them attractive tools for deconvolving the complex x-ray and gamma-ray spectra from radioactive material related to the nuclear fuel cycle.[2] However, the total photon count rate demonstrated by the instrument[2] is still modest: about 10^3 counts per second across the array and about 4 counts per second per element compared to 40×10^3 counts per second for a germanium sensor with a shaping time near 2 μs. The count rate of microcalorimeter sensors is limited by the recovery time of individual elements. For these devices,[2] the dominant 1/e thermal recovery time is $\sim$2 ms but a longer $\sim$10 ms time constant is also present. When a second photon is absorbed before a TES has been cooled to its quiescent state after an initial absorption event, the energy of the second event is difficult to determine because the resulting pulse shape differs from the quiescent response. The most direct solution to this challenge is to shorten the response time of the sensors by changes in their thermal circuit such as increasing the thermal conductance to the surrounding thermal bath. However, device speeds are invariably constrained by the capability of the readout SQUID system, and thus cannot be increased without limit.

Traditional processing maximizes signal-to-noise ratio by convolving pulse records with filters constructed from the average pulse shape and the noise power spectral density.[3,4] Spectacular degradation of performance occurs, however, when pulses are piled-up,[5] distorting pulse shape; consequently pulse processing approaches to allow operation at high count rates are an active topic of research.[6–9] Here, we introduce a filtering approach that preserves spectral resolution even when the pulse to be filtered clearly falls on the tail of the preceding pulse. The new framework departs from prior algorithms in two respects: (1) noise autocovariance replaces its mathematical dual, the noise power spectral density, to avoid the discrete Fourier transform and (2) the filter optimization is subject to explicit constraints beyond maximization of signal-to-noise ratio for isolated pulses, including for the filter length, orthogonality to constants, and orthogonality to exponentials of one or more decay rates. We evaluate and demonstrate the filters' efficacy with pulse pile-up where detector nonlinearity effects are small.

Assumed signal is a pair of pulses sitting on baseline $f(t) = a_0 s(t - t_0) + a_1 s(t - t_1) + b$, where s is the pulse shape, a_0 and a_1 are the pulse amplitudes, t_0 and t_1 are the pulse arrival times with $t_0 < t_1$, and b is the baseline. A noisy signal is $m(t) = f(t) + \eta(t)$, where the noise η realizes a stationary stochastic process. Readout electronics obtain a discrete approximation m_i of $m(i\delta)$ for i an integer, where δ is the sample time spacing. We define f_i, s_i, and η_i analogously. Our measurement model is then

$$\begin{aligned} m_i &= f_i + \eta_i \\ &= a_0 s_{i-i_0} + a_1 s_{i-i_1} + b + \eta_i. \end{aligned} \tag{1}$$

In this approximate model, pulse arrival times $t_0 = i_0\delta$, $t_1 = i_1\delta$ are assumed aligned with the sample grid, and known, to avoid interpolation issues. The pulse shape $s = (s_0, \ldots, s_n, \ldots)^t$ is approximated by averaging many pulses to obtain the estimate $\hat{s} = (\hat{s}_0, \ldots, \hat{s}_n, \ldots)^t$, normalized so $\max \hat{s} = 1$, and the noise autocovariance $r = (r_0, \ldots, r_n, \ldots)^t$, given by the expectation $r_k = \mathbb{E}[\eta_i \eta_{i+k}] - \mathbb{E}[\eta_i]^2 = \mathbb{E}[\eta_i \eta_{i+k}]$, is approximated by averaging products of pulse-free samples of the sensor output to obtain the estimate $\hat{r} = (\hat{r}_0, \ldots, \hat{r}_n, \ldots)^t$.

The standard procedure assumes $a_0 = 0$, computes discrete convolution $(q \star m)_i = \sum_{j=0}^{n-1} q_j m_{i-j}$ of a given filter

$q = (q_0, \ldots, q_{n-1})^t$ with $\ldots, m_{-1}, m_0, m_1, \ldots$, the discrete convolution of q with $\ldots, \hat{s}_{-1}, \hat{s}_0, \hat{s}_1, \ldots$, where $\hat{s}_i = 0$ for $i < 0$, and estimates a_1 as the ratio of their maximums

$$\hat{a}_1 = \frac{\max_i (q \star m)_i}{\max_i (q \star \hat{s})_i}. \tag{2}$$

We seek the mean and variance of the amplitude estimate $\hat{a}_1$. We have

$$\mathbb{E}[(q \star m)_i] = a_0 \cdot (q \star s)_{i-i_0} + a_1 \cdot (q \star s)_{i-i_1} + b \sum_{j=0}^{n-1} q_j. \tag{3}$$

We define $\bar{\imath}$ so that $(q \star s)_{\bar{\imath}} = \max_i (q \star s)_i$. Under assumptions of orthogonality to the prior tail and to constants, $(q \star s)_{\bar{\imath}+i_1-i_0} = 0 = \sum_{j=0}^{n-1} q_j$, we have

$$\mathbb{E}[\hat{a}_1] = \frac{\mathbb{E}[\max_i (q \star m)_i]}{\max_i (q \star \hat{s})_i} \approx \frac{\max_i \mathbb{E}[(q \star m)_i]}{\max_i (q \star \hat{s})_i} \approx a_1, \tag{4}$$

where the approximations are equalities under somewhat restrictive conditions.

Toward a variance estimate, $\mathbb{E}[m_{i-j} m_{i-k}] = (a_0 s_{i-i_0-j} + a_1 s_{i-i_1-j} + b)(a_0 s_{i-i_0-k} + a_1 s_{i-i_1-k} + b) + r_{j-k}$, where r_{j-k} is the noise autocovariance. Now

$$\begin{aligned}
\mathrm{Var}\,[\hat{a}_1] &= \mathbb{E}\big[\hat{a}_1^{\,2}\big] - \mathbb{E}[\hat{a}_1]^2 \\
&= \frac{\mathbb{E}\big[\max_i (q \star m)_i^2\big] - \mathbb{E}[\max_i (q \star m)_i]^2}{\max_i (q \star \hat{s})_i^2} \\
&\approx \frac{\max_i \mathbb{E}\big[(q \star m)_i^2\big] - \max_i \mathbb{E}[(q \star m)_i]^2}{\max_i (q \star \hat{s})_i^2} \\
&= \frac{q^t R q}{[q^t \overline{s}]^2} \approx \frac{q^t \hat{R} q}{[q^t \overline{s}]^2} \stackrel{\text{def}}{=} \hat{\mathrm{V}}\mathrm{ar}\,[\hat{a}_1],
\end{aligned} \tag{5}$$

where the variance estimate $\hat{\mathrm{V}}\mathrm{ar}\big[\hat{a}_1\big]$ is defined to be the last expression, $\hat{R}$ is the $n \times n$ estimated covariance matrix with $\hat{R}_{jk} = \hat{r}_{j-k} = \hat{r}_{|j-k|}$, and $\overline{s} = (\hat{s}_i, \hat{s}_{i-1}, \ldots, \hat{s}_{i-n+1})^t$ is the length n segment from $\hat{s}$ with $q^t \overline{s} = \max_i (q \star \hat{s})_i$.

Variance minimization, with orthogonality to constants or exponentials of particular decay rates, can be imposed by Lagrange optimization. For orthogonality to k vectors $V = [v_1 \cdots v_k]$, we have

$$\Lambda(q, \lambda, \gamma) = q^t \hat{R} q - \lambda [q^t \overline{s} - 1] - q^t V \gamma,$$

where λ (for unit response) and $\gamma = (\gamma_1, \ldots, \gamma_k)^t$ comprise $k + 1$ Lagrange multipliers. The solution is

$$q = \hat{R}^{-1} \overline{V} (\overline{V}^t \hat{R}^{-1} \overline{V})^{-1} e_1, \quad \hat{\mathrm{V}}\mathrm{ar}[\hat{a}_1] = q^t \hat{R} q, \tag{6}$$

where $\overline{V} = [\overline{s}\ v_1 \cdots v_k]$ and $e_1 = (1, 0, \ldots, 0)^t$ is of length $k + 1$. Figure 1 illustrates the principle of these filters. Avoidance of the discrete Fourier transform (DFT), with an increase in filter computation cost that is very mild for filter lengths up to $n \approx 10^4$, avoids false assumptions of signal and noise periodicity and yields nonperiodic filters.

Measurements at NIST of photons from a ^{153}Gd source were made with a single TES microcalorimeter,[2] at varied count rates (1.29, 2.13, 5.62, and 13.15 Hz), by placing the source at four different distances from the detector. At the highest rate, 60 267 pulses were triggered and 47 820 were filtered, after eliminating 7610 for record overlap, 3648 for SQUID mode unlock, and 1189 for other pulse shape anomalies. The following analysis focuses on pulses near the 97.431 keV gamma-ray emission line of ^{153}Gd.

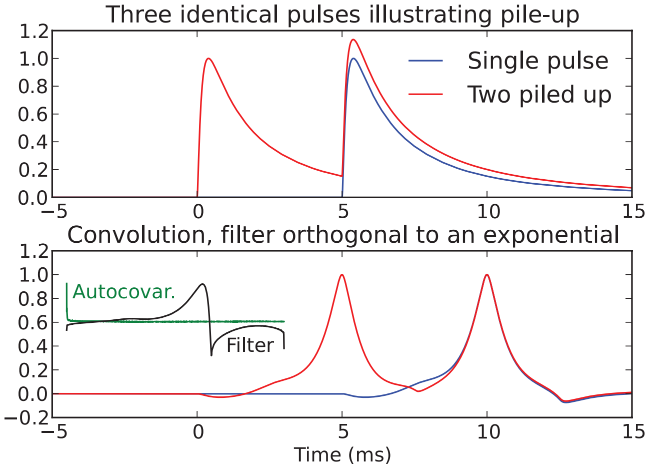

FIG. 1. Two scenarios, one with pile-up, are shown (top). From the pulse shape and noise autocovariance, a 7.5 ms filter orthogonal to an exponential of tail decay, $\tau = 3.2$ ms, is computed (inset, separate vertical scales). Convolution of the filter with the signal yields peaks of essentially constant height (bottom) and nearly eliminates pile-up dependence.

The noise spectrum and the DFT of the average pulse are used to compute the standard filter. The autocovariance and the average pulse (shown above in Fig. 1) are used to compute the proposed filters and the predicted energy resolution of each. Figure 2 shows predicted resolution versus filter length for the proposed filters and the standard DFT-computed optimal filter, with the lowest frequency bin set to zero to reduce sensitivity to baseline drift. The standard filter and the proposed filter orthogonal to constants would agree, absent discretization and periodicity artifacts due to the DFT. This calculation is for isolated pulses; for piled-up pulses these two filters suffer bias problems that are significantly reduced by the filters orthogonal to exponentials. The filter orthogonal to two exponentials, however, due to the additional constraint, suffers significant loss of sensitivity at short to moderate filter lengths, and is not considered further here. The performance of the other three filters is compared on measured pulses, and histograms near the 97.431 keV line are plotted for the highest

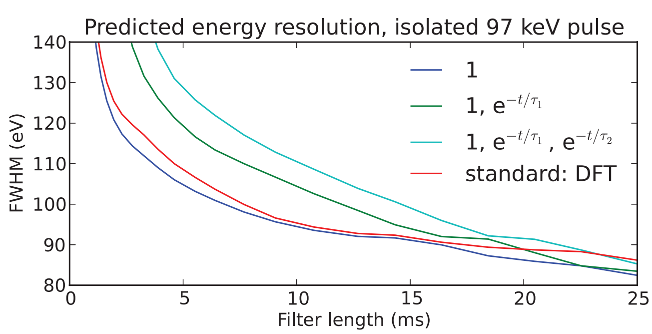

FIG. 2. Predicted resolution on an isolated pulse of four filters is shown. The filters, determined from average pulse shape and noise autocovariance, include the standard DFT-computed filter with lowest frequency bin set to zero[5] and proposed filters orthogonal to constants and zero, one, or two exponentials ($\tau_1 = 6.0$ ms, $\tau_2 = 1.5$ ms).

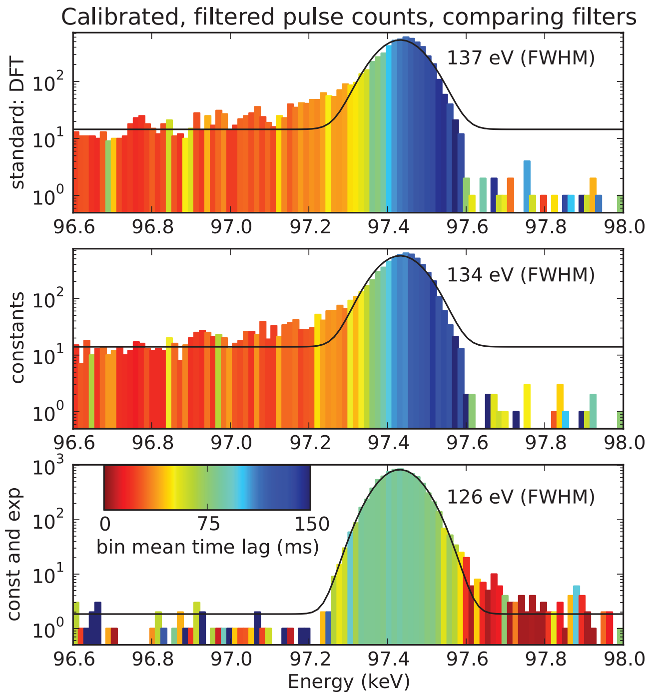

FIG. 3. Energy histograms near the 97.431 keV line, from the 13.15 Hz dataset with 10.24 ms record length, are shown for the standard filter, the proposed filter orthogonal to constants, and the proposed filter orthogonal to constants and exponentials ($\tau = 6$ ms). The third filter yielded 7515 pulses in the interval 97.431 ± 0.100 keV. Color denotes the pulse arrival time lag since the previous pulse, averaged over the histogram bin, and illustrates that filtering errors, concentrated in heavily piled-up pulses, are dramatically reduced by the filter orthogonal to exponentials.

pulse rate in Fig. 3. Each histogram was fit with a Gaussian plus, a constant to determine the energy resolution.

In Fig. 4, the output pulse rate, for the energy range 97.431 ± 0.100 keV, and energy resolution are compared for all four input count rates and the three types of filter, for both short and long pulse records. At the highest rate and for short pulse records, the filter orthogonal to both constants and exponentials ($\tau = 6$ ms) offers 45% higher output rate than the standard DFT-computed filter and 40% higher than the filter orthogonal to constants alone, at better energy resolution than either one.

We gratefully acknowledge support from the NIST Innovations in Measurement Science program, the DOE Office of Nuclear Nonproliferation Research and Development, and the DOE Office of Nuclear Energy.

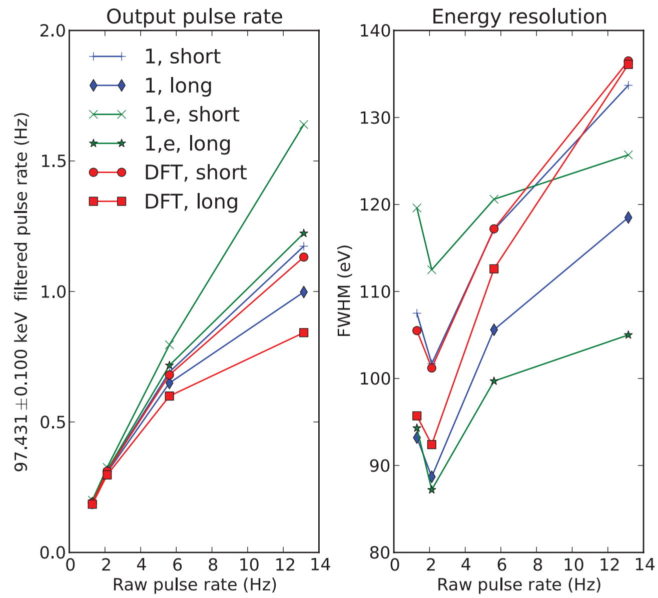

FIG. 4. The output pulse rate and energy resolution are compared across input count rates and three filter types ($\tau = 6$ ms), for both short (10.24 ms) and long (25.60 ms) pulse records. We note that the maximum output pulse rate is considerably lower than the corresponding raw pulse rate, because many raw pulses are due to spectral features other than the 97.431 keV line.

[1] M. K. Bacrania, A. S. Hoover, P. J. Karpius, M. W. Rabin, C. R. Rudy, D. T. Vo, J. A. Beall, D. A. Bennett, W. B. Doriese, G. C. Hilton, R. D. Horansky, K. D. Irwin, N. Jethava, E. Sassi, J. N. Ullom, and L. R. Vale, IEEE Trans. Nucl. Sci. **56**, 2299 (2009).
[2] D. A. Bennett, R. D. Horansky, D. R. Schmidt, A. S. Hoover, R. Winkler, B. K. Alpert, J. A. Beall, W. B. Doriese, J. W. Fowler, C. P. Fitzgerald, G. C. Hilton, K. D. Irwin, V. Kotsubo, J. A. B. Mates, G. C. O'Neil, M. W. Rabin, C. D. Reintsema, F. J. Schima, D. S. Swetz, L. R. Vale, and J. N. Ullom, Rev. Sci. Instrum. **83**, 093113 (2012).
[3] A. E. Szymkowiak, R. L. Kelley, S. H. Moseley, and C. K. Stahle, J. Low Temp. Phys. **93**, 281 (1993).
[4] S. H. Moseley, R. L. Kelley, R. J. Schoelkopf, A. E. Szymkowiak, D. McCammon, and J. Zhang, IEEE Trans. Nucl. Sci. **35**, 59 (1988).
[5] W. B. Doriese, J. S. Adams, G. C. Hilton, K. D. Irwin, C. A. Kilbourne, F. J. Schima, and J. N. Ullom, AIP Conf. Proc. **1185**, 450–453 (2009).
[6] H. Tan, D. Breus, W. Hennig, K. Sabourov, W. K. Warburton, W. B. Doriese, J. N. Ullom, M. K. Bacrania, A. S. Hoover, and M. W. Rabin, IEEE Nucl. Sci. Symp. Conf. Record **1–9**, 1130–1133 (2008).
[7] H. Tan, D. Breus, W. Hennig, K. Sabourov, J. W. Collins, W. K. Warburton, W. B. Doriese, J. N. Ullom, M. K. Bacrania, A. S. Hoover, and M. W. Rabin, AIP Conf. Proc. **1185**, 294 (2009).
[8] H. Tan, W. Hennig, W. K. Warburton, W. B. Doriese, and C. A. Kilbourne, IEEE Trans. Appl. Supercond. **21**, 276 (2011).
[9] B. K. Alpert, W. B. Doriese, J. W. Fowler, and J. N. Ullom, J. Low Temp. Phys. **167**, 582 (2012).